7

On the Impact of Time-Resolved Boundary Conditions on the Simulation of Surface Ozone and PM10

Gabriele Curci
Dept. Physics, CETEMPS, University of L'Aquila
Italy

1. Introduction

The grid-spacing of chemistry-transport models (CTM) is always limited by computational resources and ranges from 100-200 km of global scale models, to 25-50 km of continental scale models, to 1-10 km of regional and local scale models. We push to higher resolution in hope of better reproducing small scale processes that affect our ability to assess the environmental and health impacts of emissions. Running simulations at a resolution less than 50 km is often feasible only using a limited area model, which uses a domain ascribed to the region of interest. However, even the air quality of a single city is in principle affected by all the emission sources at global level: we thus account for such long-range transport of pollutants and oxidants specifying the chemical state of the atmosphere outside the domain through boundary conditions (BC). BC concentrations are usually taken from typical profiles or from larger-scale simulations with a procedure called "nesting". In this chapter, we focus on the latter technique, exploring in particular the effect of different BC time-resolutions (monthly to hourly) on the simulation of ozone and particulate matter on a nested domain at European scale. For the sake of completeness, we point out here that even very high-resolution models cannot explicitly simulate processes at all possible spatial-temporal scales and thus a certain degree of parameterization is always required. For further insights on the "subgrid" issues we refer the reader to the literature (e.g. Galmarini et al., 2008; Qian et al., 2010; Denby et al., 2011; Paoli et al., 2011).

In addition to boundary conditions, chemistry-transport model simulations also require initial conditions (IC) for chemical species. The general aspects of the influences of IC and BC on the simulation may be understood in the simplified framework presented by Liu et al. (2001). The authors consider an Eulerian box model with one chemical species, whose evolution of concentration C is regulated by the species continuity equation:

$$\frac{\mathrm{d}C}{\mathrm{d}t} = P - LC + \frac{C_{BC} - C}{\tau_r} \tag{1}$$

where P and L are the production and loss rates, respectively, C_{BC} is the background concentration, which represent the boundary condition in this case, and τ_r is the residence

time into the box. The third term on the right-hand side isolates the source term attributable to the BC. The analytical solution of the equation is as follows (eq. 4 in Liu et al., 2001):

$$C(t) = C_{IC}\, e^{-(L+1/\tau_r)t} + \frac{P\tau_r}{L\tau_r + 1}\left(1 - e^{-(L+1/\tau_r)t}\right) + \frac{C_{BC}}{L\tau_r + 1}\left(1 - e^{-(L+1/\tau_r)t}\right) \quad (2)$$

where C_{IC} is the initial condition. The influence of C_{IC} exponentially decreases with time, due both to photochemical loss and deposition (L) and outward-transport ($1/\tau_r$), thus it vanishes if a sufficient "spin-up" time is allowed. On the other hand, the importance of local sources (second term on the r.h.s.) and boundary conditions (third term on the r.h.s.) grow with time and drive the evolution of C after the "spin-up" time. The importance of BC is to be evaluated comparing the relative magnitudes of the local production term $P\tau_r$ (photochemical plus emission) against C_{BC}. If the local sources are much larger than C_{BC}, the influence of BC might be ignored. It is expected that boundary influence decreases during downwind transport and that it reaches a maximum when the arrival time is short and the species lifetime is long.

The simple considerations about the influence of IC and BC obtained from the solution in equation (2) of the box model, was demonstrated to be valid also for full three-dimensional Eulerian chemistry-transport models. Regarding IC, Berge et al. (2001) found that their influence a 3-D model decreases more slowly with time with respect to a box model, but still is reduced to <10% in the planetary boundary layer (PBL) after 3 days in a 400 km × 480 km domain covering Southern California. However, the same authors pointed out that the influence of IC might be >10% after 3 days for long lived grouped species (e.g. sum of reservoir species of ozone) and in the free troposphere. A similar spin-up time of 2 days for ozone in the PBL was reported by Jiménez et al. (2007) for a 272 km × 272 km covering North-Eastern Iberian Peninsula. On a larger domain covering Europe, Langmann & Bauer (2002) found that 5 days are needed by ozone in the PBL to "forget" its initial condition. More recently, a further sensitivity test at the North American continental scale, confirmed that a week is the minimum spin-up time recommended for a 3-D simulation of ozone and particulate matter (Samaali et al., 2009).

Liu et al. (2001) analyzed the influence of BC on their 3-D ozone simulation over California using the difference of concentrations between a reference run and another with zeroed boundary concentrations. They found that the percentage of ozone concentration attributable to BC is mostly determined by the distance from the domain edges, the influence being inversely proportional to the distance. The influence at a specific location and time is modulated by the characteristics of the local and upwind sources. During night the impact of BC on ozone is less than daytime, because of a less active photochemistry. It was calculated that BC may contribute 30-40% of ozone formation in polluted PBL, while stratospheric BC dominated ozone values in the free troposphere (Langmann & Bauer, 2002; Song et al., 2008). Barna & Knipping (2006) pointed out that a different representation of BC has a great impact on source-apportionment analysis.

While Liu et al. (2001) helped clarifying the general concepts of the influence of BC on chemistry-transport model simulations, several other studies focused on the impact of improved boundary conditions on simulations. Many studies found that increasing both temporal and spatial resolution of BC benefit the ozone (Langmann et al., 2003; Appel et al., 2007; Song et al., 2008; Szopa et al., 2009), carbon monoxide (Tang et al., 2007; Tombrou et

al., 2009) and particulate matter simulation (Barna & Knipping, 2006; Borge et al., 2010). On the continental scale, BC have a significant impact on ozone background levels, while having much less impact on the variability and peak values (Tang et al., 2007; Szopa et al., 2009). In the free troposphere, a careful treatment of the variable tropopause is critical for a real advantage in using improved stratospheric ozone BC on model top (Lam and Fu, 2009; Makar et al., 2010).

The chapter is organized as follows. We first briefly describe the models used in the study in section 2. Then we study the impact and time scales of IC and BC on simulated ozone in section 3.1. In the same section, we analyse the difference among surface ozone simulations with the use of boundary conditions alternatively with monthly, daily or hourly update rate. In section 3.2 we analyse the effect of alternative BC on surface PM10, in particular during a Saharan dust event in July 2005. The scientific questions we shall try to address are:

- How long should be the spin-up time for simulated surface concentrations to be unaffected by initial conditions?
- How much is the contribution of boundary conditions to local ozone and PM10 levels?
- Is there any improvement in simulations of ozone and PM10 if the boundary conditions are provided at an higher frequency (up to the model time-step)?

In final section 4 we draw conclusions on these questions.

2. Models description

In this section we give a brief description of chemistry-transport models used in this study. We use the CHIMERE regional model (Bessagnet et al., 2008) to simulate lower atmosphere composition over continental Europe and the GEOS-Chem global model (Bey et al., 2001) to provide CHIMERE with gases and dust boundary conditions.

2.1 CHIMERE regional model

CHIMERE is a regional chemistry-transport model developed by a community of French institutions primarily designed to produce daily forecasts of ozone, aerosols and other pollutants and make long-term simulations for emissions control scenarios (Bessagnet et al., 2008; CHIMERE, 2011). In this study, The model is setup on a 0.5°×0.5° horizontal grid covering Europe (35°-58°N; 15°W-25°E) and 8 hybrid-sigma vertical layers extending to 500 hPa. Meteorological input is provided by PSU/NCAR MM5 model (Dudhia, 1993) run at 36×36 km² horizontal resolution and 29 vertical sigma layers extending up to 100 hPa, and regridded on the 0.5° × 0.5° CHIMERE grid. The model is forced by NCEP analyses using the grid nudging (grid FDDA) option implemented in MM5.

Anthropogenic emissions are derived from the Co-operative Programme for Monitoring and Evaluation of the Long-range Transmission of Air pollutants in Europe (EMEP) annual totals (Vestreng, 2003) for NOx, CO, VOC, SOx, NH3 and primary PM species, while carbonaceous aerosol emissions are taken from Junker & Liousse (2008). Biogenic emissions of isoprene and monoterpenes are calculated with the MEGAN model (Guenther et al., 2006). Dust and sea-salt emissions are also simulated on-line (CHIMERE, 2011).

The gas-phase chemical mechanism MELCHIOR (Latuatti, 1997) includes about 50 species and 120 reactions. The aerosol phase is simulated with a sectional approach with 8 size bins

from 0.04 to 10 μm of diameter. The main processes governing the production and loss of main inorganic (sulphate, nitrate, ammonium) and organic secondary species are included.

Boundary conditions are implemented in a classical one-way approach. Species concentrations at the boundaries are introduced in the simulation through an outer envelope of model cells having the same resolution of the actual simulation grid. The boundary concentrations are transported inside the domain by the transport operator, i.e. the part of the model that simulates advection (Fig. 1). Regardless of the particular scheme choice (CHIMERE, 2011), the model uses information only from one upwind cells to solve for advection. Numerical stability is warranted by the adaptive time-step adjusted in order to have a Courant number always less than 1, e.g. for the zonal direction:

$$C_x = U \cdot \Delta t / \Delta x \tag{3}$$

where C_x is the Courant number for the x-direction, U is the maximum zonal wind speed, Δt is the time step, and Δx is the grid spacing. By definition, the Courant number measures the influence that upwind concentrations may have on a given grid-cell in a single time-step in units of the grid size. If this number is less than one it means that information from only one upwind cell is needed. In CHIMERE, the time-step is adapted throughout the simulation to ensure this condition always holds. For some more details on the relationship among advection schemes and boundary conditions the reader is referred to the nice discussion given by Wang et al. (2004).

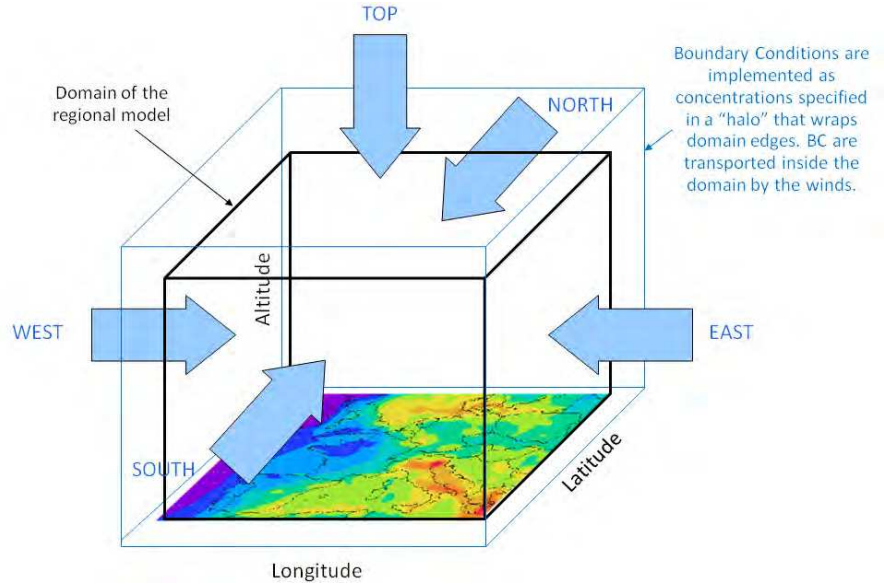

Fig. 1. Schematic of boundary conditions (BC) of a regional chemistry-transport model. The domain of simulation is denoted by the black cube, the 2-D map at the bottom is a sample of an output surface ozone field. Boundary concentrations of gases and aerosol species are passed to the model through an envelope of cells that wraps the domain around its edges. The transport operator of the model will use those cells for advection calculations and it will transport BC information into the domain.

In the default configuration, the boundary conditions for CHIMERE regional simulations are taken from monthly mean simulations of the global model LMDz-INCA (Hauglustaine et al., 2004) for species listed in Tab. 1. For aerosol species, size-resolved mass concentrations of global model are redistributed onto regional model size bins, using a simple linear interpolation in logarithmic bin diameters space. In Fig. 2 we show a sample of the monthly static ozone boundary conditions for the month of June.

CHIMERE species	**Species long name**	**GEOS-Chem species**
Gases		
O3	Ozone	O3
NO2	Nitrogen dioxide	NO2
HNO3	Nitric acid	HNO3
PAN	Peroxyacetylnitrate	PAN
H2O2	Hydrogen peroxide	H2O2
CO	Carbon monoxide	CO
CH4	Methane	-
HCHO	Formaldehyde	CH2O
C2H6	Ethane	C2H6
NC4H10	Butane and higher alkanes	ALK4
C2H4	Ethene	-
C3H6	Propene	PRPE
OXYL	Xylenes	-
Aerosol		
H2SO4	Sulfates	-
OC	Organic Carbon	-
BC	Black Carbon	-
DUST	Dust	DST1-4
SS	Sea Salts	-

Table 1. List of species for which boundary conditions are provided to CHIMERE regional chemistry-transport model. In the third column, the GEOS-Chem global model species used in this study to test sensitivity of CHIMERE to different boundary conditions.

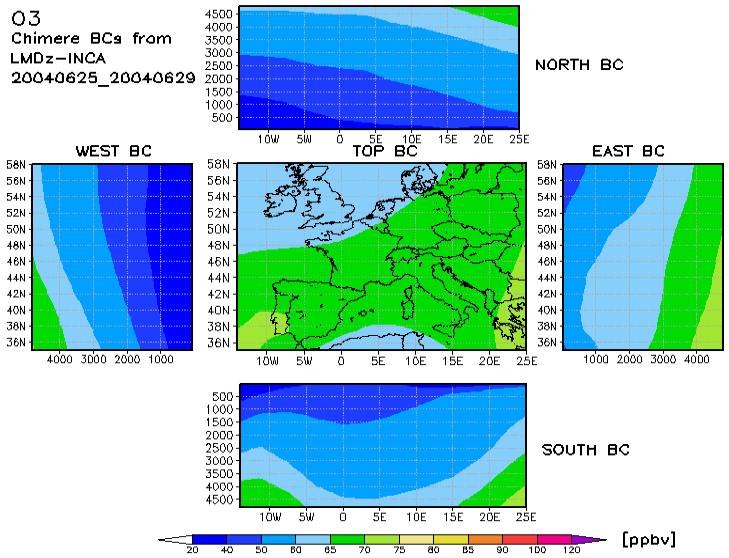

Fig. 2. Sample default ozone boundary conditions of CHIMERE model for the month of June. Ozone concentrations are taken from the monthly average of a simulation of the LMDz-INCA global model (Hauglustaine et al., 2004) and interpolated upon the CHIMERE horizontal and vertical grids. The panels show the resulting concentrations at the sides and top lid of the domain, as if the "box" of Fig. 1 has been open on a table.

2.2 GEOS-Chem global model

GEOS-Chem is a global chemistry model developed by a large international users community, originally stemming from the Harvard's Atmospheric Chemistry Modelling group (Bey et al., 2001; GEOS-Chem, 2011). The meteorological input is provided by the Goddard Earth Observing System (GEOS) of the NASA Global Modeling and Assimilation Office (GMAO). Mostly relevant to this study is the emission module developed by Fairlie et al. (2007), used here to include a more detailed contribution of Saharan dust emissions into the simulations. Desert dust emissions are lowered by a factor of three according to the study of Generoso et al. (2008).

GEOS-Chem simulations will be used in this study to produce alternative boundary conditions for the CHIMERE regional model at different time scales, from hourly to monthly.

3. Results

3.1 Ozone

3.1.1 Time-scales and impact of IC and BC

In order to study the effect of initial and boundary conditions on the CHIMERE ozone simulation at the European scale we use the simulations listed in Tab. 2. Basically, we alternatively zero IC and BC to isolate their effect through the difference with a reference

simulation (Stein & Alpert, 1993). We choose a one month in summer (June 2005) in order to allow enough time to study the effect of IC and to ensure an active ozone photochemistry.

Simulation Label	Description
CTRL	Control simulation (reference)
NIC	No Initial Conditions (IC = 0)
NBC	No Boundary Conditions (BC = 0)

Table 2. List of simulations performed to study the effect of initial and boundary conditions on ozone.

The reference ozone simulation of CHIMERE is quickly evaluated against ground based measurements available from the EMEP network (www.emep.int). Let Obs_i^j and Mod_i^j be the observed and modeled values at time i and station j, respectively. Let N be the number of stations, and $Nobs^j$ the number of observations at station j.

- Pearson's Correlation (r) and coefficient of determination (R^2):

$$r = \frac{1}{N}\sum_{j=1}^{N}\frac{1}{Nobs^j - 1}\sum_{i=1}^{Nobs^j} Z_i^j(Mod)\cdot Z_i^j(Obs)$$
$$Z(X) = \frac{X - \langle X \rangle}{\sigma_X} \tag{4}$$

where X is a generic vector and $Z(X)$ is its standard score, also defined above. R^2 is defined as the square of r and denotes the fraction of variability of observations explained by the model.

- Mean Bias (MB):

$$MB = \frac{1}{N}\sum_{j=1}^{N}\left(\frac{1}{Nobs^j}\sum_{i=1}^{Nobs^j} Mod_i^j - Obs_i^j\right) \tag{5}$$

- Mean Normalized Bias Error (MNBE):

$$MNBE = \frac{1}{N}\sum_{j=1}^{N}\left(\frac{1}{Nobs^j}\sum_{i=1}^{Nobs^j}\frac{Mod_i^j - Obs_i^j}{Obs_i^j}\right)\times 100 \tag{6}$$

- Mean Normalized Gross Error (MNGE):

$$MNGE = \frac{1}{N}\sum_{j=1}^{N}\left(\frac{1}{Nobs^j}\sum_{i=1}^{Nobs^j}\frac{\left|Mod_i^j - Obs_i^j\right|}{Obs_i^j}\right)\times 100 \tag{7}$$

Results for current simulation are presented in Tab. 3 and Fig. 3. The model captures the central part of the observed distribution, but overestimates its low end and underestimates the upper end. This is a quite typical behaviour of regional chemistry-transport models (e.g. Appel et al., 2007). The average MNBE and MNGE for ozone hourly timeseries is slightly

above the quality thresholds recommended by EPA (15% and 35% respectively), but the indices are well within the suggested limits for the daily maxima timeseries.

Variable	Observed mean	Modelled mean	MB	MNBE	MNGE	r
Units	$\mu g/m^3$	$\mu g/m^3$	$\mu g/m^3$	%	%	
O3 hourly	78.6	82.7	4.0	22.5	36.5	0.53
O3 daily max	103.4	98.7	-4.7	-0.4	15.8	0.69

Table 3. Comparison of observed and modelled ozone timeseries at EMEP monitoring stations. Values are averaged over all times and stations available for June 2005.

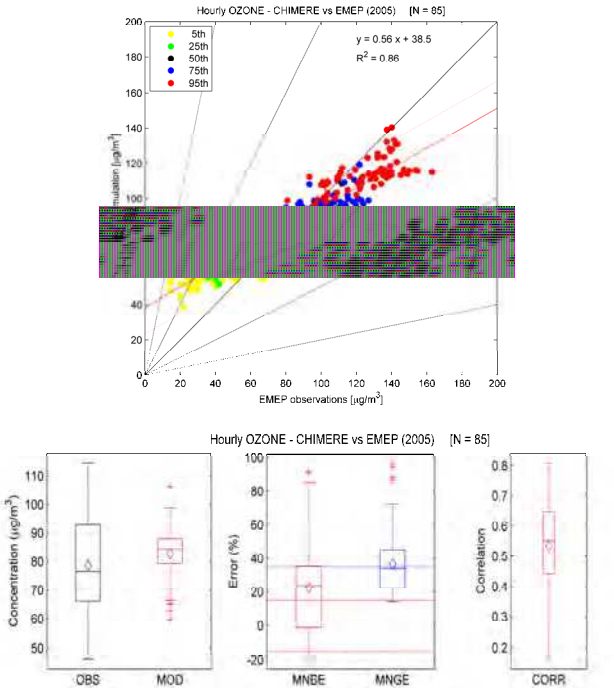

Fig. 3. Comparison of hourly ozone observed and modelled at EMEP stations. Left panel: scatter plot of 5th, 25th, 50th, 75th and 95th percentiles at all available stations. Right panel: boxplot of statistical indices shown in Tab. 3. Horizontal reference lines denote the quality level suggested by EPA (1991).

The impact of IC on ozone is studied through the difference between CTRL and NIC runs. We arbitrarily define the influence of Ψ_{IC} as the relative difference between CTRL and NIC simulations and the spin-up time τ_{IC} as the time needed to reduce Ψ_{IC} to less than 1%. In Fig. 4 we show the average ozone timeseries as measured and modelled at EMEP stations. After about 4 days of simulations the average Ψ_{IC} becomes negligible. According to our definition

the average τ_{IC} is 3.9 days, but ranges from 0.5 to 8.1 days. In Fig. 5 we may appreciate the spatial distribution of τ_{IC}. We find a clear positive gradient from the North-West to the South-East of the domain. The reason may be found in the ozone distribution itself. In Fig. 6 we show the average ozone concentrations simulated by the model and we note that τ_{IC} gradients follows closely ozone gradients: the model just takes more time to build up ozone from the zero concentration starting point when the ozone level to be reached is higher. While this may pose questions on the method we used to estimate the "lifetime" of IC, this test is useful to verify that the model is essentially able to completely forget a whatever "wrong" initial condition after about 9 days of run.

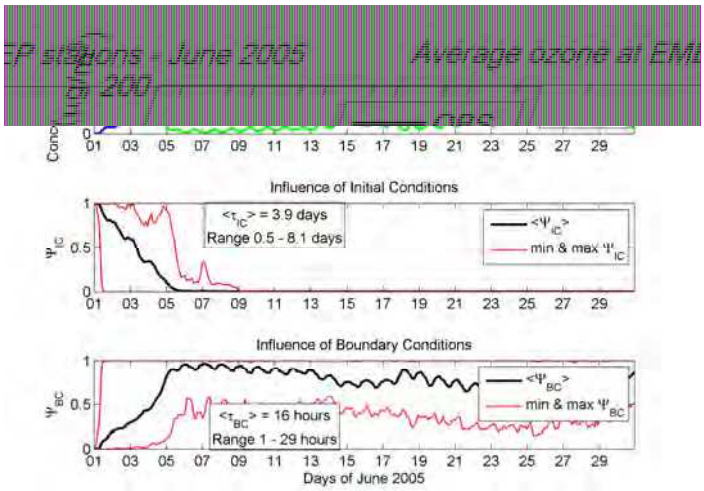

Fig. 4. Simulated influence of initial (IC) and boundary conditions (BC) in CHIMERE ozone at the European scale. The average timeseries at EMEP monitoring stations are shown. For explanation of simulation labels please refer to Tab. 2. The definition of Ψ_{IC}, Ψ_{BC}, τ_{IC}, and τ_{BC} is given in main text.

The influence of boundary conditions is studied in an analogous way. We define Ψ_{BC} as the difference between CTRL and NBC runs and the time of arrival of BC τ_{BC} as the first time when Ψ_{BC} is larger than 1%. In Fig. 4 we see that the behaviour of Ψ_{BC} mirrors that of Ψ_{IC}. As expected, the influence of BC grows as that of IC decreases. According to our definition, the average τ_{BC} is 16 hours, and ranges from 1 to 29 hours. As shown in Fig. 5, shortest times are found near the domain edges, while longest times are found in the interior of the domain. The variability inside the domain is attributable to the specific meteorological situations, since the time of arrival of BC at a specific location is determined by the winds encountered along the travel from the edges.

Until the spin-up time (τ_{IC}) is elapsed, Ψ_{BC} continues to ramp until a plateau is reached: the model is "warmed-up", and the ozone production at certain place is determined by the equilibrium between the sources inside the domain and the boundary conditions (eq. 2). For any time and location, Ψ_{BC} quantifies the relative influence of BC with respect to local production. The periods with higher values of Ψ_{BC} in timeseries of Fig. 4, thus indicate periods of less intense photochemical activity.

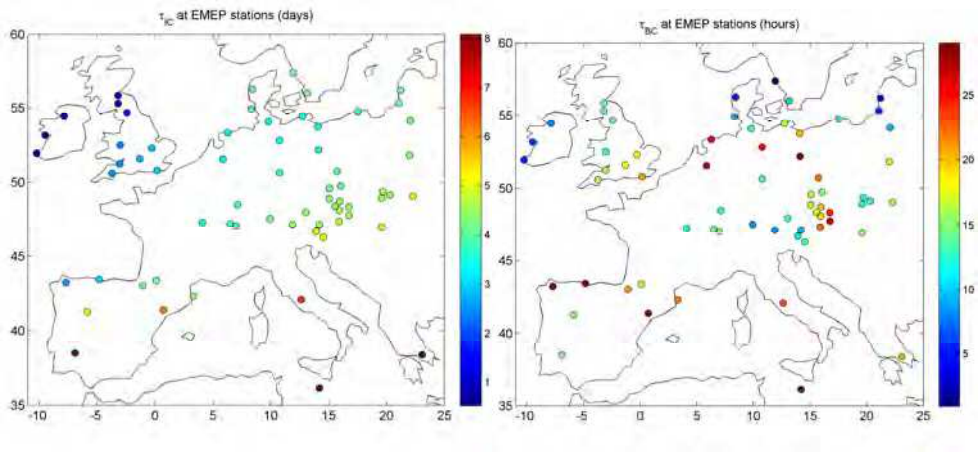

Fig. 5. Spatial distribution of the influence time of IC and BC on ozone.

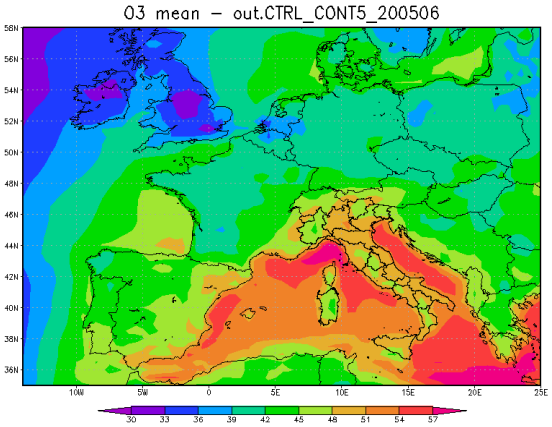

Fig. 6. Average surface ozone simulated with CHIMERE in June 2005.

The spatial distribution of the average Ψ_{BC} at the surface calculated from 10 to 30 June 2005 with CHIMERE is shown in Fig. 7. As also noted above, we find that the maximum influence of BC is around the borders, and it is striking to see that it is higher than 80-90% even in the polluted North-Western Europe. Ψ_{BC} reaches a minimum of less than 50% over Po Valley where the local production is invigorated by the elevated precursors emissions and very active photochemistry. This result imply that an error in BC may be effectively propagated into the simulation domain. For example, an error of 1 in the BC becomes 0.7 in a place where $\Psi_{BC} = 0.7$.

Liu et al. (2001) found that 3-D model results are consistent with analytical solution of a simple one-dimensional model, where the influence of BC may be written as:

$$\psi_{BC} = C_{BC} e^{-Lx/u} S_{x/u}(t) \tag{8}$$

where x is the distance to boundary and u is the wind speed, so that x/u is the time of BC arrival. S is a step function which is 0 for $t < x/u$ (before BC arrival) and 1 for $t \geq x/u$ (after BC arrival). If the ozone lifetime $\tau = 1/L$ is known, equation (8) can be applied directly to estimate Ψ_{BC}. Since the lifetime is generally unknown, but the BC arrival time τ_{BC} can be easily estimated, equation (8) can be inverted to roughly estimate the local averaged ozone lifetime. Inserting our definition of *relative* influence of BC on ozone Ψ_{BC} we obtain:

$$\tau = -\tau_{BC} / \log(\psi_{BC}) \tag{9}$$

The result is shown in Fig. 7. Ozone lifetime estimated with this simple method ranges 1-3 days in the continental boundary layer and is longer than 5 days over the ocean, which is quite consistent with our expectations.

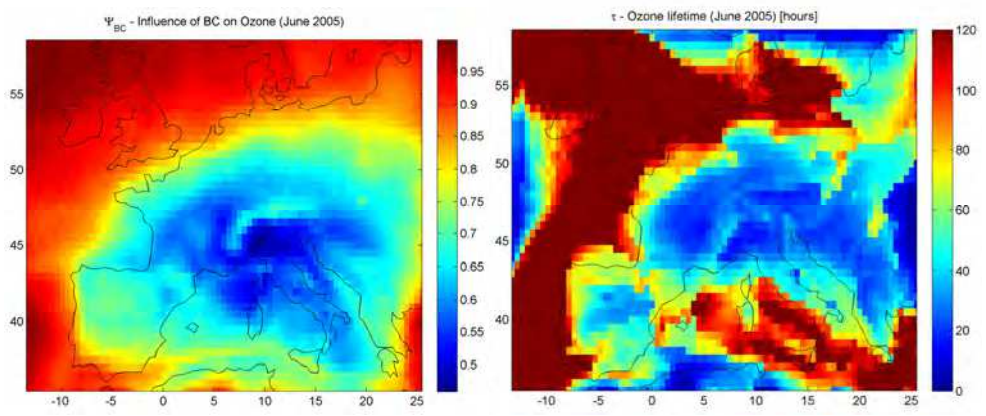

Fig. 7. Left: average influence of BC on ozone simulated in June 2005 (excluding first 9 days of spin-up). Right: ozone lifetime estimated with eq. 9.

3.1.2 Effect of alternative BC on surface ozone

We analyse the effect of different BC on simulated surface ozone using four simulations as listed in Tab. 4. We choose a longer summer period of two months, June and July 2005, to have a more robust statistics. Consistently with what found in previous section, we spin-up the model for 10 days.

Simulation Label	Description
CTRL	Control simulation (w/ reference LMDz-INCA BC)
BCGM	BC from GEOS-Chem monthly output
BCGD	BC from GEOS-Chem daily output
BCGH	BC from GEOS-Chem hourly output

Table 4. List of simulations performed to study the effect of alternative boundary conditions on ozone.

In Fig. 8 we compare the timeseries of ozone BC in the simulations averaged over the western border (leftmost rectangle in Fig. 2). The GEOS-Chem model simulates lower (higher) ozone

values with respect to LMDz-INCA in June (July). One important reason, apart the many differences in models' formulation, is that the latter simulation is an average over five years of run, while GEOS-Chem simulates the "actual" (i.e. assimilated) meteorology of the CHIMERE simulation. The introduction of more detailed in time BC introduces much more variability, with differences up to ±30% with respect to the fixed monthly BC.

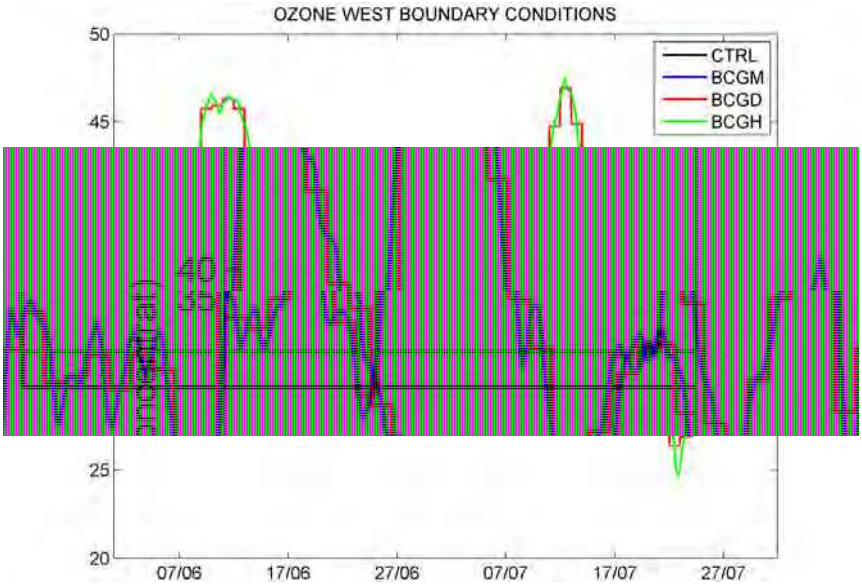

Fig. 8. Timeseries of the ozone boundary condition averaged over the west side of the European domain (left side of the box in Fig. 2). For explanation of the simulation labels please refer to Tab. 4.

In Tab. 5 we report the statistical summary, i.e. the average indices over all available EMEP stations, of the four simulations. The comparison with reference simulation over the two-month period is consistent with the one month simulation without spin-up (Tab. 3). The introduction of GEOS-Chem BC benefits the high CHIMERE model bias, reducing both the normalized bias and the gross error, probably because they are more specific of the simulation period than the LMDz-INCA climatology. The introduction of time resolution into the BC produces further reduction of model error and also significantly increases the correlation with the measurements.

Simulation	Observed mean	Modelled mean	MB	MNBE	MNGE	r
Units	$\mu g/m^3$	$\mu g/m^3$	$\mu g/m^3$	%	%	
CTRL	77.6	81.5	3.9	28.0	42.3	0.55
BCGM	77.6	77.2	-0.3	20.8	38.9	0.56
BCGD	77.6	75.4	-2.2	16.9	36.8	0.59
BCGH	77.6	75.3	-2.6	13.1	33.4	0.58

Table 5. Statistical indices of sensitivity simulations against EMEP hourly ozone measurements for June-July 2005. Values are averaged over all times and stations available.

In Fig. 9 we compare the simulated ozone with measurements at two selected EMEP stations, one near the border and very sensitive to BC (Mace Head, Ireland), the other about the centre of the domain and much less sensitive to BC (Heidenreichstein, Austria). For the Irish site we note interesting differences among the runs. During the first week of simulation, the monthly GEOS-Chem alternative BC enhances model underestimation with respect to reference, while the time-resolved GEOS-Chem BC slightly alleviates the bias with respect to reference. In the days around June 17th the time-resolved BC allow the model to capture a low ozone episode, but the subsequent week GEOS-Chem values are even too low. Also in other periods, the time-resolved BC allow the model to go closer to observations (July 7-10, 20-23). The correlation with measurements goes from 0.38 of the CTRL run, to 0.29 of the BCGM, to 0.44 of BCGD and BCGH. The gross error is reduced from 26% to 22% from CTRL to BCGD and BCGH runs. We also point out that the difference of the impact of hourly and daily BC is minimal.

The effect of alternative BC on the Austrian site, as expected is much less evident. However, the statistical indices of comparison with observation constantly get better as we introduce more resolution in time. The correlation increases from 0.56 to 0.61, the bias decreases from 23% to 14%, and the gross error decreases from 39% to 35%. Again, we note that using hourly or daily resolved BC does not significantly impact the simulation.

These results point out that the time resolution of BC may greatly affect the simulation, but an higher resolution may episodically worsen model skills. The big step is between monthly and daily resolved BC, while going down to hourly resolved BC, at the expense of more disk space and pre-processing time, does not yield further significant improvements..

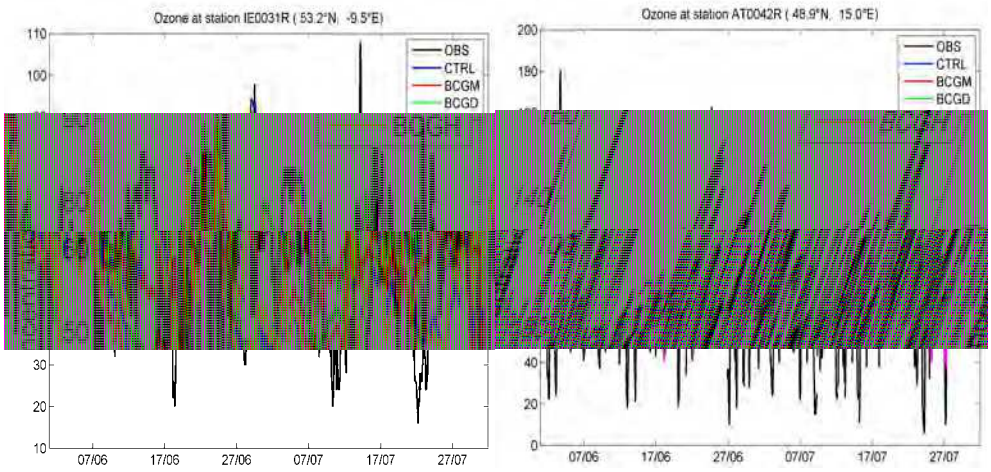

Fig. 9. Ozone timeseries in June-July 2005 as observed at two EMEP stations and simulated with CHIMERE with four sensitivity simulations (Tab. 4). Left: Mace Head station, close to the Western border of the domain and sensitive to BC (Ψ_{BC} ~0.95). Right: Heidenreichstein station, by the centre of the domain and less sensitive to BC (Ψ_{BC} ~0.63).

3.2 Aerosol

3.2.1 Effect of alternative BC on surface PM10

Similarly to ozone, we study the effect of alternative BC on simulated surface PM10 using the same simulations listed in Tab. 4. For this study, we choose to introduce alternative BC into CHIMERE only for dust, because the inflow of Saharan dust into the European domain is expected to contribute much more to the PM10 simulation than the other species (Curci et al., 2008; Curci & Beekmann, 2007). While transboundary pollution from anthropogenic sources is expected to impact background levels of PM (Park et al., 2003; 2004), Saharan dust may episodically yield to the exceedance of the PM10 limit for the protection of human health of 50 μg/m³ (Gobbi et al., 2007; Koçak et al., 2007; Perrino et al., 2009). It is estimated that in Italy the subtraction of natural dust to PM10 may yield to a reduction from 5% to 50% of the number of threshold exceedances depending on the meteorology and the station type (Pederzoli et al., 2010).

In Fig. 10 we compare the boundary conditions to CHIMERE from the Southern border in the four simulations. GEOS-Chem monthly mean dust values are higher than LMDz-INCA, and similarly to ozone the time-resolved BC have a much higher variability, with differences of ±50% and one episode with hourly values three times higher than monthly values.

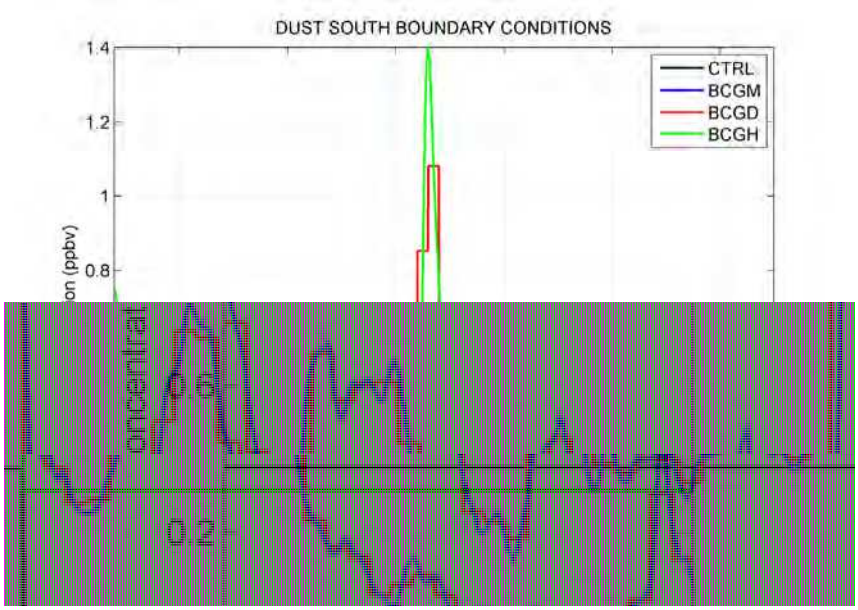

Fig. 10. Timeseries of the dust boundary condition summed over all CHIMERE size-bins and averaged over the south side of the European domain (bottom side of the box in Fig. 2). For explanation of the simulation labels please refer to Tab. 4.

In Tab. 6 we report the average statistical indices over all available EMEP stations of the four simulations. The higher dust values in GEOS-Chem BC drastically reduce the model bias from -40% to -7%, but the "noise" introduced by the large dust variability gradually

degrades the correlation and the gross error as we increase the BC time resolution. This fact points out how tricky is the simulation of the Saharan dust contribution on European PM10 levels.

Simulation	Observed mean	Modelled mean	MB	MNBE	MNGE	r
Units	$\mu g/m^3$	$\mu g/m^3$	$\mu g/m^3$	%	%	
CTRL	17.5	9.0	-8.5	-41.9	47.4	0.63
BCGM	17.5	15.1	-2.4	-8.6	42.8	0.53
BCGD	17.5	16.0	-1.5	-6.9	50.2	0.50
BCGH	17.5	16.0	-1.5	-7.0	50.3	0.50

Table 6. Statistical indices of sensitivity simulations against EMEP daily PM10 measurements for June-July 2005. Values are averaged over all times and stations available.

In Fig. 11 we compare the PM10 timeseries at two EMEP stations, one near the South-Western border of the domain and more affected by Saharan dust (Barcarrota, Spain), and another to the North (Schauinsland, Germany). At the Spanish site, higher dust values in GEOS-Chem BC reduces the mean bias from -14 $\mu g/m^3$ to less than 1 $\mu g/m^3$, but the correlation decreases from 0.77 to 0.56 in CTRL and BCGH runs, respectively. The better resolved BC allow the model to better capture the observed PM10 variability by the end of the simulated period, but they also induce episodic overshoots during the first period of simulation that are completely unrealistic. Very similar features may be also noted at the German site, indicating that the importance of dust BC are not limited to the Southern part of the European domain.

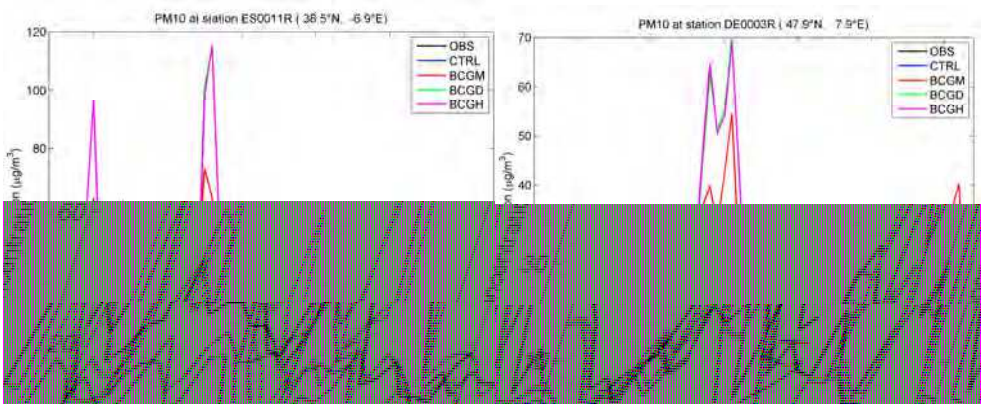

Fig. 11. PM10 timeseries in June-July 2005 as observed at two EMEP stations and simulated with CHIMERE with four sensitivity simulations (Tab. 4). Left: Barcarrota station, close to the South-Western border of the domain and strongly impacted by Saharan dust. Right: Schauinsland station, by the centre of the domain.

We now focus on the dust episode of 27-29 July 2005. In Fig. 12, the daily AOD observed by MODIS/Aqua between 24-29 July clearly tracks a dust cloud swapping Southern Europe from West to East. In Fig. 13 we show the same episode as recorded at ground level by the EMEP network and simulated by CHIMERE. The introduction of time-resolved BC helps the

model in better reproducing both timing and magnitude of the event. Unfortunately, as we have seen in previous timeseries, this is not a general conclusions and further work is certainly warranted on the dust BC issue.

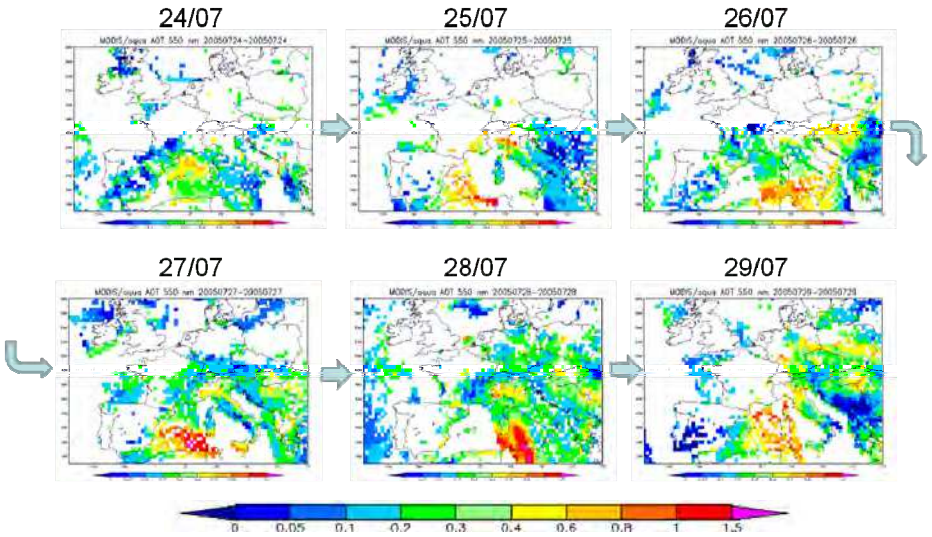

Fig. 12. The Saharan dust episode of July 2005 as seen from space through daily Aerosol Optical Depth (AOD) observations by MODIS/Terra.

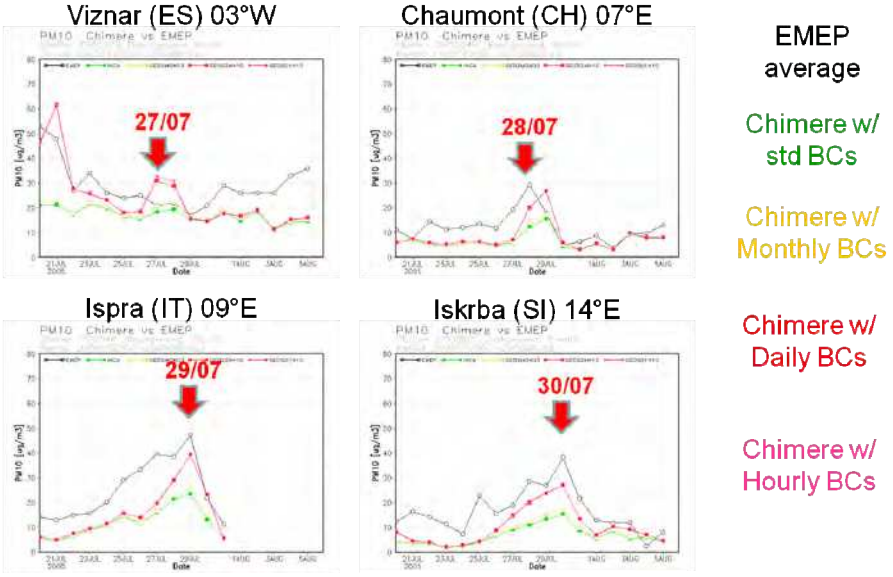

Fig. 13. The dust episode observed at EMEP stations and simulated with CHIMERE using different time-resolutions for the boundary conditions.

3.2.2 Eye-witness of a Saharan dust event over Central Italy

In a sort of "divine intervention", Sahara desert decided to produce one of its episodes while writing this chapter, during the first days of September 2011. The event was eye-witnessed by the author, and by its fellow citizens of L'Aquila in Central Italy, during the days 2-4. A large "bubble" of dust travelled over the South-Western Mediterranean and it was captured by the MODIS/Terra satellite instrument, as depicted in Fig. 14, which estimated a maximum optical thickness of more than 1.5. In Fig. 15 we show the striking effect on atmospheric visibility as observed from the ground: the mountain peak by the centre of the pictures, having a distance of about 25 km from the shot location, was almost obscured by the dust layer. The latter did actually hit the ground, as witnessed by the PM10 monitoring station in L'Aquila valley, which exceeded 50 $\mu g/m^3$ on September 3rd (Fig. 16), and also by the dust deposited over surfaces at the ground (e.g. the author's car depicted in Fig. 15).

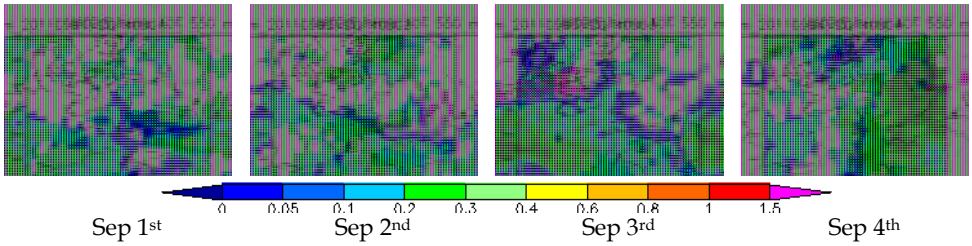

Fig. 14. The Saharan dust event over Italy in September 2011 as seen from MODIS/Terra AOD observations.

Fig. 15. Left: view of L'Aquila valley in a clean summer day (10/09/2011); the mountain peak in the centre is at a distance of about 25 km. Middle: same view during a Saharan dust event (03/09/2011). Right: dust deposited over ground surfaces during the night.

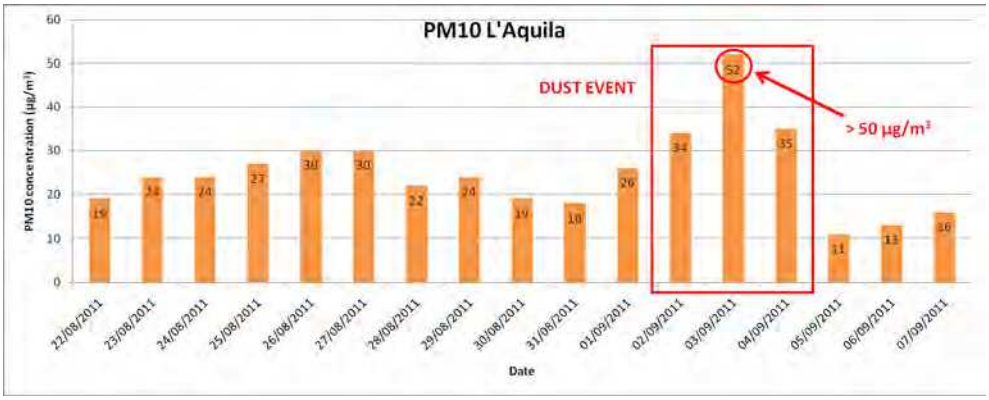

Fig. 16. PM10 concentration measured in L'Aquila at the ground monitoring station across the September 2011 Saharan dust event.

Interestingly, Fig. 17 shows that the arrival of the dust layer was qualitatively predicted by the ForeChem experimental chemical weather forecast system operating at University of L'Aquila (Curci, 2010), consisting of MM5/CHIMERE models automatically running, which is fed with the default monthly boundary conditions from LMDz-INCA global model (see Sec. 2.1).

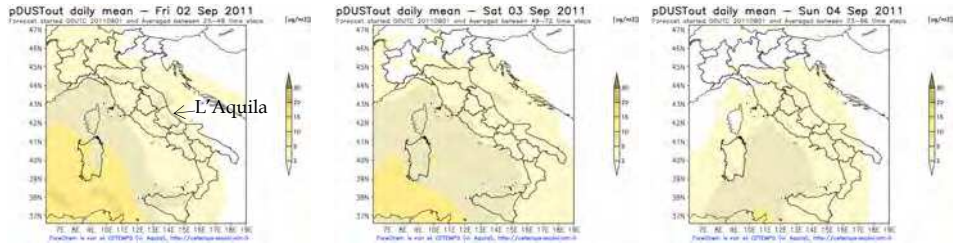

Fig. 17. Saharan dust event over Italy in September 2011 as forecasted with MM5/CHIMERE (ForeChem experimental chemical weather forecast operational at University of L'Aquila, http://pumpkin.aquila.infn.it/forechem/). Images show the fraction of PM10 at the ground due to dust from outside the domain, which is a nest within a European scale domain. Boundary conditions to the latter are provided with monthly mean fields from the LMDz-INCA global model.

4. Conclusion

The effect of initial (IC) and boundary conditions (BC) on the simulation of surface ozone and PM10 over the continental scale European domain is evaluated with several sensitivity tests of the CHIMERE chemistry-transport model.

Zeroing alternatively IC and BC in the model, and comparing the results with a reference run, we estimate an optimal model spin-up time of 9 days for the domain used in this study (35°-58°N; 15°W-25°E; 79 x 47 cells at 0.5° horizontal resolution). The BC have a significant

impact on simulated ozone, especially in a belt of about 1000-2000 km around the domain borders. There, BC dominates ozone variability, while in the interior of the domain they have a weight similar to the local photochemical production. Through the BC test, the surface ozone lifetime is estimated to be 1-3 days over the continent and longer than 5 days over the oceans.

The impact of different time-resolution of BC is studied feeding the CHIMERE model with GEOS-Chem global model simulations. With respect to the reference BC, provided by five years monthly mean LMDz-INCA model simulations, the GEOS-Chem model has generally lower ozone and enhanced dust values during the period of simulation (June-July 2005). The positive ozone bias with respect to EMEP measurements is alleviated by GEOS-Chem BC, and also the introduction of BC better resoled in time benefit model skills. The average correlation increases from 0.55 to 0.59 and the normalized bias decreases from 28% to 17%. The large improvement is noticed when passing from monthly to daily BC, while hourly BC do not produce further improvements. We noticed, however, that time-resolved BC may episodically worsen model skills.

The introduction of different aerosol BC is tested focusing on dust, because of the prominent role that Saharan dust events play on the PM10 levels especially in Southern Europe. GEOS-Chem predicts higher dust concentrations with respect to LMDz-INCA, and its use as BC alleviates the CHIMERE low bias with respect to EMEP measurements. However, the agreement with observations get better during the events by the end of the simulated period (July 2005), but worsen at the beginning (June 2005). In particular, GEOS-Chem has a tendency to episodically overshooting dust at unrealistic levels. The introduction of time-resolved dust BC may allow the model to better reproducing both time and magnitude of Saharan events, but this is not a general conclusion with models' set-up used in this study. Further work on dust BC for European scale models is certainly needed in the future, possibly combining satellite observations with ground measurements of the aerosol composition and size-distribution that may better constrain the dust contribution to particulate matter.

5. Acknowledgment

The author was supported by the Italian Space Agency (ASI) in the frame of QUITSAT and PRIMES projects.

6. References

All figures in this chapter are originals by the author.

Appel, K. W.; Gilliland, A. B.; Sarwar, G. & Gilliam, R. C. (2007). Evaluation of the Community Multiscale Air Quality (CMAQ) model version 4.5: Sensitivities impacting model performance Part I—Ozone. *Atmospheric Environment*, Vol.41, pp. 9603–9615

Barna, M. G. & Knipping, E. M. (2006). Insights from the BRAVO study on nesting global models to specify boundary conditions in regional air quality modeling simulations. *Atmospheric Environment*, Vol.40, pp. S574–S582

Berge, E.; Huang, H.-C.; Chang, J. & Liu, T.-H. (2001). A study of the importance of initial conditions for photochemical oxidant modeling. *Journal of Geophysical Research*, Vol.106, pp. 1347-1363

Bessagnet, B.; Menut, L.; Curci, G.; Hodzic, A.; Guillaume, B.; Liousse, C.; Moukhtar, A.; Pun, B.; Seigneur, C. & Schulz, M. (2008). Regional modeling of carbonaceous aerosols over Europe - Focus on Secondary Organic Aerosols. *Journal of Atmospheric Chemistry*, Vol.61, pp. 175-202

Bey, I.; . Jacob, D. J.; Yantosca, R. M.; Logan, J. A.; Field, B.; Fiore, A. M.; Li, Q.; Liu, H.; Mickley, L. J. & Schultz, M. (2001). Global modeling of tropospheric chemistry with assimilated meteorology: Model description and evaluation. *Journal of Geophysical Research*, Vol.106, pp. 23073-23096

Borge, R.; López, J.; Lumbreras, J.; Narros, A. & Rodríguez, E. (2010). Influence of boundary conditions on CMAQ simulations over the Iberian Peninsula. *Atmospheric Environment*, Vol.44, pp. 2681-2695

CHIMERE (2011). The CHIMERE chemistry-transport model User's Guide, Available from: http://www.lmd.polytechnique.fr/chimere/chimere.php

Curci, G. (2010). An Air Quality Forecasting tool over Italy (ForeChem). In: *Proceedings of 31st Technical Meeting on Air Pollution Modelling and its Application*, Torino, Italy, Sep 2010

Curci, G. & Beekmann, M. (2007). Contribution of natural and biogenic emissions to the Air Quality in Europe. In: *NatAir final activity report,* pp. 141-175, Available from http://natair.ier.uni-stuttgart.de/NatAir_Final_Activity_Report.pdf

Curci, G.; Beekmann, M.; Vautard, R.; Bessagnet, B.; Menut, L.; Smiatek, G. ; Steinbrecher, G.; Theloke, J. & Friedrich, R. (2008). Impact of updated European biogenic emission inventory on air quality using Chimere chemistry-transport model. *IGAC 10th International Conference, Bridging the scales in Atmospheric Chemistry : Local to Global*, Annecy, France, September 7-12, 2008, Available from http://pumpkin.aquila.infn.it/gabri/downld/curci_igac2008_bioPM.pdf

Denby, B.; Cassiani, M.; de Smet, P.; de Leeuw, F. & Horálek, J. (2011). Sub-grid variability and its impact on European wide air quality exposure assessment. *Atmospheric Environment*, Vol.45, pp. 4220-4229

Dudhia, J. (1993). A nonhydrostatic version of the Penn State/NCAR mesoscale model: Validation tests and simulation of an Atlantic cyclone and cold front. *Monthly Weather Review*, Vol.121, pp. 1493–1513

EPA (1991). Guideline for regulatory application of the urban airshed model. U.S. Environmental Protection Agency, Office of Air Quality Planning and Standards, July 1991, 108 pp.

Fairlie, T. D.; Jacob, D. J. & Park, R. J. (2007). The impact of transpacific transport of mineral dust in the United States. *Atmospheric Environment*, Vol.41, pp. 1251-1266

Galmarini, S.; Vinuesa, J.-F. & Martilli, A. (2008). Modeling the impact of sub-grid scale emission variability on upper-air concentration. *Atmospheric Chemistry and Physics*, Vol.8, pp. 141-158

Generoso S.; Bey I.; Labonne M. & Breon F. M. (2008). Aerosol vertical distribution in dust outflow over the Atlantic: Comparisons between GEOS-Chem and Cloud-Aerosol Lidar and Infrared Pathfinder Satellite Observation (CALIPSO). *Journal of Geophysical Research*, Vol.113, D24209

GEOS-Chem (2011). The GEOS-Chem User's guide, Available from: www.geos-chem.org.

Gobbi, G. P.; Barnaba, F. & Ammannato, L. (2007). Estimating the impact of Saharan dust on the year 2001 PM10 record of Rome, Italy. *Atmospheric Environment,* Vol.41, No.2, (January 2007), pp. 261-275

Guenther, A.; Karl, T.; Harley, P.; Wiedinmyer, C.; Palmer, P. I. & Geron, C. (2006). Estimates of global terrestrial isoprene emissions using MEGAN (Model of Emissions of Gases and Aerosols from Nature). *Atmospheric Chemistry and Physics*, Vol.6, pp. 3181-3210

Hauglustaine, D. A.; Hourdin, F.; Walters, S.; Jourdain, L.; Filiberti, M.-A.; Larmarque, J.-F.; & Holland, E. A. (2004). Interactive chemistry in the Laboratoire de Météorologie Dynamique general circulation model: description and background tropospheric chemistry evaluation. *Journal of Geophysical Research*, Vol.109, D04314

Jiménez, P.; Parra, R. & Baldasano, J. M. (2007). Influence of initial and boundary conditions for ozone modelling in very complex terrains: A case study in the northeastern Iberian Peninsula. *Environmental Modelling & Software*, Vol.22, pp. 1294-1306

Junker, C. & Liousse, C. (2008). A global emission inventory of carbonaceous aerosol from historic records of fossil fuel and biofuel consumption for the period 1860–1997. *Atmospheric Chemistry and Physics*, Vol.8, pp. 1195–1207

Lam, Y. F. & Fu, J. S. (2009). A novel downscaling technique for the linkage of global and regional air quality modelling. *Atmospheric Chemistry and Physics*, Vol.9, pp. 9169–9185

Koçak, M.; Mihalopoulos, N. & Kubilay, N. (2007). Contributions of natural sources to high PM10 and PM2:5 events in the eastern Mediterranean. Atmospheric Environment Vol.41, 3806–3818

Langmann, B. & Bauer, S. E. (2002). On the Importance of Reliable Background Concentrations of Ozone for Regional Scale Photochemical Modelling. *Journal of Atmospheric Chemistry*, Vol.42, pp. 71–90

Langmann, B.; Bauer, S. E. & Bey, I. (2003). The influence of the global photochemical composition of the troposphere on European summer smog, Part I, Application of a global to mesoscale model chain. *Journal of Geophysical Research*, Vol.108, 4146 (14 pp.)

Lattuati, M. (1997). Contribution à l'étude du bilan de l'ozone troposphérique à l'interface de l'Europe et de l'Atlantique Nord: Modélisation lagrangienne et mesures en altitude, *Ph.D. thesis*, Univ. Pierre et Marie Curie, Paris, France

Liu, T.-H.; Jeng, F.-T.; Huang, H.-C. ; Berge, E. & Chang, J. S. (2001). Influences of initial conditions and boundary conditions on regional and urban scale Eulerian air quality transport model simulations. *Chemosphere – Global Change Science*, Vol.3, pp. 175–183

Makar, P. A.; Gong, W.; Mooney, C.; Zhang, J.; Davignon, D.; Samaali, M.; Moran, M. D.; He, H.; Tarasick, D. W.; Sills, D. & Chen, J. (2010). Dynamic adjustment of climatological ozone boundary conditions for air-quality forecasts. *Atmospheric Chemistry and Physics*, Vol.10, pp. 8997-9015

Paoli, R.; Cariolle, D. & Sausen, R. (2011). Review of effective emissions modeling and computation. *Geoscientific Model Development*, Vol.4, pp. 643-667

Park, R. J.; Jacob, D. J., Chin, M. & Martin, R. V. (2003). Sources of carbonaceous aerosols over the United States and implications for natural visibility. Journal of Geophysical Research, Vol.108, pp. 4355

Park, R. J.; Jacob, D. J., Field, B. D., Yantosca, R. M. & Chin, M. (2004). Natural and transboundary pollution influences on sulfate-nitrate-ammonium aerosols in the United States: Implications for policy, Journal of Geophysical Research, Vol.109, D15204

Pederzoli, A.; Mircea, M.; Finardi, S.; di Sarra, A. & Zanini G. (2010). Quantification of Saharan dust contribution to PM10 concentrations over Italy during 2003-2005. *Atmospheric Environment*, Vol.44, pp. 4181-4190

Perrino, C.; Canepari, S.; Catrambone, M.; Dalla Torre, S.; Rantica, E. & Sargolini, T. (2009). Influence of natural events on the concentration and composition of atmospheric particulate matter. *Atmospheric Environment*, Vol.43, pp. 4766-4779

Qian, Y.; Gustafson Jr., W. I. & Fast, J. D. (2010). An investigation of the sub-grid variability of trace gases and aerosols for global climate modelling. *Atmospheric Chemistry and Physics*, Vol.10, pp. 6917-6946

Samaali, M.; Moran, M. D. ; Bouchet, V. S. ; Pavlovic, R. ; Cousineau, S. & Sassi, M. (2009). On the influence of chemical initial and boundary conditions on annual regional air quality model simulations for North America. *Atmospheric Environment*, Vol.43, pp. 4873–4885

Song, C.-K.; Byun, D. W.; Pierce, R. B.; Alsaadi, J. A.; Schaack, T. K. & Vukovich, F. (2008), Downscale linkage of global model output for regional chemical transport modeling: Method and general performance. *Journal of Geophysical Research*, Vol.113, D08308 (15 pp.)

Stein, U. & Alpert, P. (1993). Factor separation in numerical simulations. *Journal of the Atmospheric Sciences*, Vol.50, pp. 2107-2115

Szopa, S.; Foret, G.; Menut, L & Cozic, A. (2009). Impact of large scale circulation on European summer surface ozone and consequences for modelling forecast. *Atmospheric Environment*, Vol.43, pp. 1189–1195

Tang, Y.; Carmichael, G. R.; Thongboonchoo, N.; Chai, T.; Horowitz, L. W.; Pierce, R. B.; Al-Saadi, J. A.; Pfister, G.; Vukovich, J. M.; Avery, M. A.; Sachse, G. W.; Ryerson, T. B.; Holloway, J. S.; Atlas, E. L.; Flocke, F. M.; Weber, R. J.; Huey, L. G.; Dibb, J. E.; Streets, D. G. & Brune, W. H. (2007). Influence of lateral and top boundary conditions on regional air quality prediction: A multiscale study coupling regional and global chemical transport models. *Journal of Geophysical Research*, Vol.112, D10S18 (21 pp.)

Tombrou, M.; Bossioli, E.; Protonotariou, A. P.; Flocas, H.; Giannakopoulos, C. & Dandou, A. (2009). Coupling GEOS-CHEM with A Regional Air Pollution Model for Greece. *Atmospheric Environment*, Vol.43, pp. 4793–4804

Vestreng, V. (2003). Review and revision. Emission data reported to CLRTAP, Tech. rep., EMEP MSC-W

Wang, Y. X.; McElroy, M. B.; Jacob, D. J. & Yantosca, R. M. (2004). A nested grid formulation for chemical transport over Asia: Applications to CO. *Journal of Geophysical Research*, Vol.109, D22307 (20 pp.)

Winner, D. A. & Cass, G. R. (1995). Effect of alternative boundary conditions on predicted ozone control strategy performance: A case study in the Los Angeles area. *Atmospheric Environment*, Vol.29, pp. 3451-3464

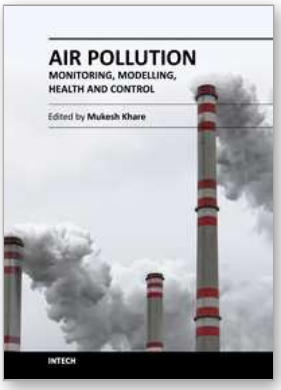

Air Pollution - Monitoring, Modelling, Health and Control
Edited by Dr. Mukesh Khare

ISBN 978-953-51-0381-3
Hard cover, 254 pages
Publisher InTech
Published online 21, March, 2012
Published in print edition March, 2012

Air pollution has always been a trans-boundary environmental problem and a matter of global concern for past many years. High concentrations of air pollutants due to numerous anthropogenic activities influence the air quality. There are many books on this subject, but the one in front of you will probably help in filling the gaps existing in the area of air quality monitoring, modelling, exposure, health and control, and can be of great help to graduate students professionals and researchers. The book is divided in two volumes dealing with various monitoring techniques of air pollutants, their predictions and control. It also contains case studies describing the exposure and health implications of air pollutants on living biota in different countries across the globe.

How to reference
In order to correctly reference this scholarly work, feel free to copy and paste the following:

Gabriele Curci (2012). On the Impact of Time-Resolved Boundary Conditions on the Simulation of Surface Ozone and PM10, Air Pollution - Monitoring, Modelling, Health and Control, Dr. Mukesh Khare (Ed.), ISBN: 978-953-51-0381-3, InTech, Available from: http://www.intechopen.com/books/air-pollution-monitoring-modelling-health-and-control/on-the-impact-of-time-resolved-boundary-conditions-on-the-simulation-of-surface-ozone-and-pm10

INTECH
open science | open minds

InTech Europe
University Campus STeP Ri
Slavka Krautzeka 83/A
51000 Rijeka, Croatia
Phone: +385 (51) 770 447
Fax: +385 (51) 686 166
www.intechopen.com

InTech China
Unit 405, Office Block, Hotel Equatorial Shanghai
No.65, Yan An Road (West), Shanghai, 200040, China
中国上海市延安西路65号上海国际贵都大饭店办公楼405单元
Phone: +86-21-62489820
Fax: +86-21-62489821